Automated control of complex aerodynamic flows generated by Windshaper fan arrays

Aurélien Walpen*, Tony Govoni†, Jonas Stirnemann‡, Matei Ionescu§, Nicolas Bosson¶, Guillaume Catry‖
WindShape, Rue de Bourgogne 25, Geneva, CH-1203, Switzerland

Flavio Noca **
University of Applied Sciences (HES-SO), Geneva, CH-1202, Switzerland

Windshapers, also known as fan-array wind generators, offer a high degree of control over complex aerodynamic flows thanks to the independent control of their thousands of small fans. But the process of setting up, measuring, and validating these flow profiles for aerodynamic tests can be time-consuming and cumbersome. In this study, a novel and intuitive approach is presented, making this process less tedious.

An optically tracked 5-hole probe was developed to collect and process three-dimensional flow data in real-time. The flow data is used in a feedback loop to precisely control each and every fan of the Windshaper to generate the desired flow profile in the test area. A 3D graphical interface allows users to set-up the flow easily and visualize how the generated flow profile might deviate from the setpoint in every area of the test section.

The present study is divided in two parts. First, we evaluated the accuracy and frequency response of the probe's flow measurement capabilities. Then, we tested the effectiveness of the flow control setup with a series of wind profiles. The results obtained demonstrate that this approach can significantly reduce the time and effort required to generate and control complex flows for aerodynamic testing.

Specifically, our tests showed that the real-time flow control method allowed to generate the desired flow profile in the test area with sufficient precision and with a short setup time. The 3D graphical interface provides an intuitive and easy-to-use platform for setting up the flow and visualizing any deviations from the setpoint. Finally, the probe's performance is up to industry standards and exceeds the requirements for precise flow control of a Windshaper.

Overall, our results suggest that this novel method provides an innovative and effective solution for generating and controlling complex aerodynamic flows, with potential applications in a range of industries including aerospace, automotive engineering, and wind energy.

I. Nomenclature

X, Y, Z	=	Laboratory's coordinate system
U, V, W	=	Flow velocity components in the x, y, z direction (laboratory's coordinate system)
U_{pr}, V_{pr}, W_{pr}	=	Flow velocity components in probe-fixed coordinates
u, v, w	=	Velocity fluctuations in the x,y,z direction
$\overline{U}, \overline{V}, \overline{W}$	=	Mean flow velocity x, y, z direction
I	=	Turbulence intensity
D	=	Probe tip diameter
d	=	Probe holes diameter
Re	=	Reynolds number

*Head of Research & Development, WindShape, aurelien.walpen@windshape.com, https://www.windshape.com
†Research & Development Engineer, WindShape, tony.govoni@windshape.com, https://www.windshape.com
‡Junior Engineer, WindShape, jonas.stirnemann@windshape.com, https://www.windshape.com
§Junior Engineer, WindShape, matei.ionescu@windshape.com, https://www.windshape.com
¶COO, WindShape, nicolas.bosson@windshape.com, https://www.windshape.com
‖CEO, WindShape, guillaume.catry@windshape.com, https://www.windshape.com
**Professor, Head of Aero-Nautical-Space group, flavio.noca@hesge.ch, https://www.hesge.ch/hepia/en/group/aero-nautical-space

Re_D	=	Probe tip Reynolds number
ρ	=	Flow density
α_{pr}	=	Pitch angle in probe-fixed coordinates
β_{pr}	=	Yaw angle in probe-fixed coordinates
α	=	Pitch angle in laboratory coordinates
β	=	Yaw angle in laboratory coordinates

II. Introduction

A. Multi-hole probe

The use of multi-hole probes to determine simultaneously the magnitude and direction of a fluid's velocity dates back to at least the 1920s [1]. Over the years, advancements in materials and manufacturing techniques [2] [3] have facilitated the development of more precise and robust multi-hole probes. Today, despite the apparition of more advanced measurement techniques providing better spatial or temporal resolution, such as hot-wire anemometry or laser doppler velocimetry, multi-hole probes are still a widely-used alternative due to their relative affordability, robustness and ease-of-use. Such probes are notably used for characterizing turbomachines [4], wind tunnel models' wakes [5] or even atmospheric flow studies [6].

In a recent advancement in multi-hole probes measurement techniques, a motion tracking system was used to track a hand-held probe in real-time with sub-millimeter accuracy [7]. The simultaneous probe flow measurement and positional data were then joined in a 3D grid and interpolated to generate a 3D time-averaged flow field of the scanned area. This system is currently commercialized under the name ProCap by the Swiss company Streamwise *.

B. Flow Control in wind tunnels

Since the inception of wind tunnels in the early 20th century [8] [9], ensuring precise and stable flow velocity within the test section has always been a fundamental requirement [10]. However, even today most subsonic wind tunnels still use open-loop controllers due to cost of a closed-loop controller and the complexity of tuning such a system [11]. Nonetheless, there has been several implementations of control systems, mainly using PID in conjunction with neural networks [12], feed-forward algorithm [13], fuzzy control [14] and genetic algorithms [15]. However, all of these methods are based on a single-point velocity measurement, assuming a uniform wind velocity profile in the test section. Doing so does not provide the means to control the wind profile itself.

There has been attempts at regulating wind profiles generated by multi-fan wind tunnels, both in 1D [16] and 2D [17], but in both cases these used flow-management devices such as honeycomb, mesh grid or contraction to homogenize the flow and also automated traverse systems to acquire data at predetermined points.

C. Windshapers

Conventional wind tunnels, developed primarily to meet the demands of the aeronautical industry [18], have certain limitations when it comes to replicating the characteristics of low-altitude atmospheric flow. These limitations stem from the low-turbulence, steady, and flat-profile winds that traditional wind tunnels generate, which are opposite to the high-turbulence, unsteady and non-homogeneous flow naturally occurring in the atmosphere. In recent years, a new class of wind generators, known as Windshapers or fan-array wind generators, has emerged to address these limitations [19]. Windshapers offer the ability to reproduce gusts and atmospheric turbulence at full-scale [20], providing a more realistic and versatile testing environment. However, the complex nature of these facilities, with their large number of fans (several thousands in some cases), poses challenges in terms of setting up specific wind profiles with precision and efficiency.

In light of these challenges and developments, this study aims to explore a novel approach that combines the advancements in multi-hole probe technology, motion-tracking, and the capabilities of Windshapers to enable the generation and precise control of varied aerodynamic flow-profiles.

*http://www.streamwise.ch/

Fig. 1 Picture of the 5-hole probe on top of a 9 x 9 x 2 fan Windshaper. The handle is visible in blue anodized aluminum, the L-shaped tube in black anodized aluminum with the reflective markers (grey spheres), and the measuring tip in light grey.

III. Experimental Setup

A. 5-hole probe

For this study, a 5-hole probe (called WindProbe) with a pyramidal tip was designed and manufactured (see Figure 1). The 5-hole tip is additively manufactured using Masked Stereolithography Apparatus (MSLA) technology with a resolution of 35 µm, which can produce precise internal holes of less than 1 mm diameter and achieve very high overall geometrical accuracy and smooth surface finish at a fraction of the cost of traditional machining techniques. The side faces are at a 90° angle to each other and its geometry, in particular its outer diameter D and hole diameter d, has been optimised to limit Re sensitivity [3] even when used at the lower end of its velocity range. The probe has a flow acceptance cone with a 40° angle.

The probe pressure measurements are conducted with ±500 Pa differential pressure sensors directly integrated in the probe handle. These temperature-compensated sensors have a total error band of less than ±0.25% of Full-Scale Span (FSS). Pressure measurements are done at a frequency of 200 Hz. The probe is also equipped with a type K thermocouple lodged inside the L-shaped tube and an absolute pressure sensor to calculate the air density ρ of the measured flow. A microcontroller unit is also integrated in the probe handle, and is running the reconstruction algorithm to output the velocity components in the probe's coordinate system (U_{pr}, V_{pr}, W_{pr}). The measurement data is then sent through serial communication to the users' computer at 200 Hz via a USB cable.

Made out of aluminum, the probe body is composed of an L-shaped tube of 100 x 270 mm covered with four motion tracking markers (12.7 mm diameter), and a handle of ⌀40 x 200 mm.

The probe was calibrated using a 324-fan Windshaper, equipped with a flow filter and a converging duct (5.2:1 contraction ratio), producing flow velocity from 2.5 - 39 m/s with a turbulence intensity of ≤0.17%. The reference velocity was measured in real-time using differential static pressure ports situated at the contraction's extremities and connected to an ISO-17025 calibrated Furness FCO-510 micromanometer (0 - 2000 Pa). The differential pressure ports were themselves calibrated beforehand using a pitot-static tube placed in the same position as the 5-hole probe. For calibration, the motion tracking system was used to determine the probe's orientation with regards to the incoming flow at a frequency of 120 Hz. The probe was then automatically rotated in every combination of pitch and yaw angle using a custom-made robotic system that keeps the probe's tip in the same point during rotation. The calibration setup is visible in the figure 2.

Due to the probe's hand held operation, a new calibration method was developed [21] to acquire calibration data in a continuous stochastic way to account for transient effects and eliminate bias from predefined acquisition patterns and mitigate hysteresis effects. This new calibration procedure was automatically repeated at several velocities covering the probe's measurement range, averaging approximately 100'000 measurement points per velocity step.

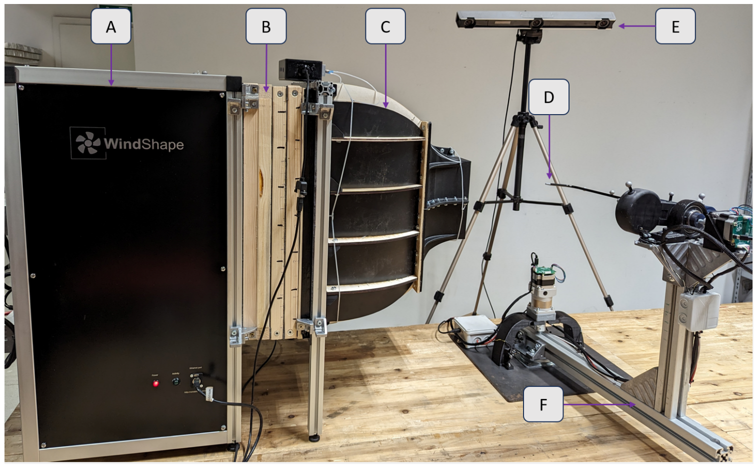

Fig. 2 Picture of the calibration setup. A: The Windshaper wind generator, B: Flow management device, C: Contraction section, D: Multi-hole Probe, E: Optitrack V120:Trio motion tracking system, F: In-house Two axis robot.

B. Windshaper

The Windshaper used to generate and measure wind profiles in the present study is composed of 80 x 80 x 86 mm fan-assemblies with two counter-rotating fans, which can be controlled independently. Each fan can generate winds from 2 - 16 m/s in steps of roughly 0.02 m/s, and with an input frequency of up to 20 Hz. The Windshaper is composed of 6 x 6 x 2 fans (72 fans in total), and was equipped with motion tracking reflecting markers (12.7 mm diameter) attached on its front face to track the Windshaper's position in the test area.

C. Control Software (WindMaster)

A new Graphical User Interface (GUI), called WindMaster, was elaborated (see Figure 3), giving users the ability to interact with a 3-dimensional virtual replica of the test area, comprising of the Windshaper and the probe. Since both objects are optically tracked, their positions are updated in real-time. The GUI allows users do all the set up actions such as defining a desired wind profile or positioning the measurement plane. The interface also brings numerous flow measurement display options in a similar way to CFD post-processing softwares: plane cut with velocity magnitude contour, velocity vectors, number of samples collected in each voxel, deviation from setpoint, etc. All these setup and display options can be changed on the fly without having to restart measurement.

The back-end of the control software works in the following way. First, the measurement space is discretized in a mesh of cubic cells with a size equal to the fan frontal area (80 x 80 mm). These cells are further subdivided in a radial-based sub-mesh (like the layers of an onion) to help provide a better averaging of the velocity across a cell. Indeed, close to the fans' exit especially, the velocity field is non-uniform across the fan area (the hub region will see a lower than average velocity, and the blade swept area will see a larger than average velocity).

The flow measurement transmitted by the WindProbe are merged with the corresponding motion tracking data, correlating each velocity vector with the position in space where the measurement was taken. Each data point is then placed inside the corresponding sub-mesh of each cell inside the discretized virtual space. Once enough points have been taken across the measurement plane, the average velocity can be calculated across each sub-mesh layer, and then the cell average can be computed as the average of each sub-mesh layer pondered by their area.

Knowing the average velocity in each cell, which correspond to the flow generated by each fan in the WindShaper, a simple P-type controller can be used to adjust the fan power input by the difference between the desired wind profile and the measured flow.

D. Motion Tracking

To collect the position of both the probe and the Windshaper in real-time, an OptiTrack V120:Trio motion tracking setup was used. This system is capable of tracking objects up to 5.25 m away at 120 Hz with sub-millimeter positioning accuracy and a latency of 8.33 ms.

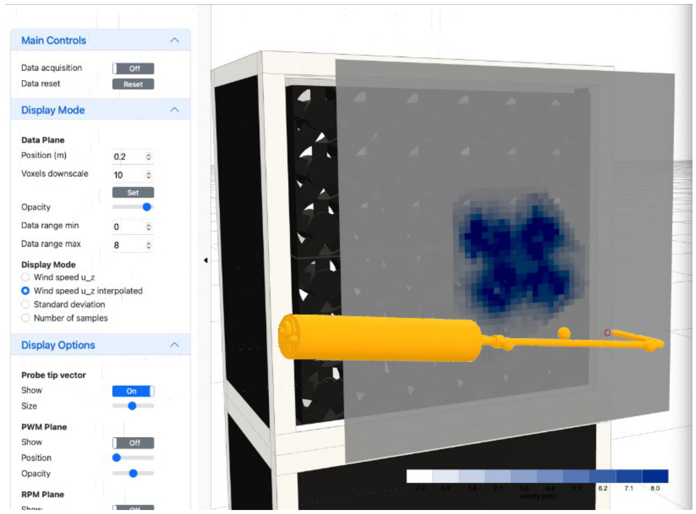

Fig. 3 Screenshot of the GUI showing the 5-hole probe (in yellow) measuring the flow profile generated by the small 6 x 6 x 2 fan Windshaper with only its 4 central fans turned on. The display plane is situated at 0.1 m downstream of the Windshaper, and the w velocity is displaed in shades of blue.

IV. Test Protocol

A. Probe Capabilities

The probe capability to accurately measure the WindShaper's flow in hand-held operation is evaluated under three main aspects: (1) the quality of the measured signal in various operation conditions, (2) the frequency response of the system, and (3) the additional error resulting from the uncontrolled displacement of the probe.

1. Flow angle and magnitude measurement error

First, the probe's measurement accuracy is assessed by exposing the probe to a steady flow with a well defined magnitude and orientation and comparing the reconstructed flow velocity calculated by the probe with the actual velocity. For this, we used the same setup previously used for calibration, allowing us to expose the probe to any flow angle within its acceptance cone as well as any flow velocity in its measurement range. From this data, one can compute a measurement error on both the velocity magnitude and flow angle.

2. Frequency Response

As the probe is operated by hand with continuous live acquisition (meaning users can move the probe rapidly across space, in and out of the flow, etc.), and is also capturing flow data at a high frequency (200 Hz), its capacity to measure transient flows accurately needs to be evaluated.

In our probe design, the pressure sensors are embedded in the handle and connected to the measurement tip through polymer tubes with an approximate length of 500mm. To ensure accurate measurements, it is essential to quantify and minimize the damping within these tubes. For this, we measure its frequency response thanks to a small apparatus comprising of an hermetically sealed box with a loudspeaker membrane attached to one end, and two pressure ports at the other extremity (see Figure 4). The first pressure port is connected to a control pressure sensor (P0), identical to the one employed in the probe. The second pressure port is replicating the probe's measurement chain by having a second sensor (P1) connected to the port via a tube identical in material and dimensions to the one connecting the probe's tip to the sensors within the handle. The loudspeaker can then be used to generate a sinusoidal pressure variation in the cavity, controlled both in frequency and amplitude. By comparing the pressure recorded by the control sensor P0 with the pressure at sensor P1 after the polymer tube, one can then quantify the impact of the tubing within the probe, and so, the frequency response of our system.

A series of measurements was conducted on different tubes with different materials, internal diameters, external diameters and lengths (see the list in Table 1). For all these tubes, a frequency sweep from 10 to 400 Hz with an

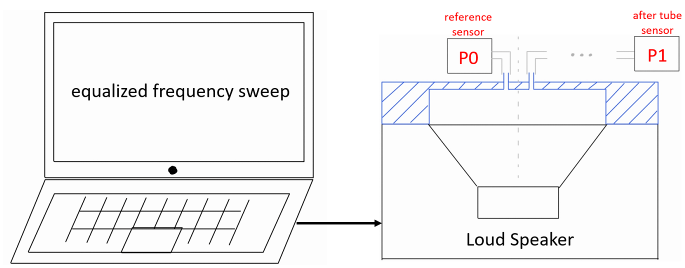

Fig. 4 Diagram of the frequency response measurement system. An hermetically sealed cavity is attached to a loudspeaker (on the right side of the image) with two pressure ports. The first one is connected to a reference pressure sensor (noted P0), and the second one is connected through a polymer tube to a second pressure sensor (noted P1), replicating the probe's tubing and sensor system. A computer (on the left side of the image) is used to drive the loudspeaker, creating pressure variations inside the cavity, which can be measured by both sensors. By performing frequency sweep equalized to a constant pressure, one can measure the polymer tubing's effect on the probe's pressure measurements.

equalized amplitude of 200 Pa (a dynamic pressure equivalent to a flow velocity of 19 m/s in Standard Temperature and Pressure (STP) conditions) was performed.

To better understand what influence the tubing attenuation could have on the flow measurements, a reference flow measurement was taken using a triple hot-wire anemometer (HWA) operated in constant temperature mode (CTA). For this, a Dantec Dynamics 55P95 probe composed of three platinum-plated tungsten wires with a dimension of 5 μm in diameter and 1.25 mm in length was used. The sensor was mounted on a Dantec Dynamics 55H27 6 mm diameter probe support and connected to a Dantec Dynamics StreamLine 90N10 CTA Frame with 1:20 bridge ratio using 4 m-long Dantec BNC cables. A National Instruments 9239 4-channel 24-Bit A/D converter was employed to convert the signals. Velocity fluctuations were sampled at 10 kHz on each channel. The HWA was calibrated in-situ using the uniform flow generated by the WindShaper equipped with a flow management device. The mean flow velocity was obtained using a Pitot-static tube connected to a Furness FCO-510 precision micromanometer by averaging its results over 30 measurements. Moreover, the flow temperature was measured using a Bosch BME280 temperature, humidity and pressure sensor.

A reference flow measurement was conducted with the WindShaper running at 95% PWM on all fans, and the CTA probe positioned 1.5 m downstream at the fan area's center. This reference measurement, representative of the "true" wind velocity variation, is then used as an input for a simulation of the WindProbe's measurement capabilities. This simulation incorporates the attenuation profile of the tubing and the sampling frequency of the pressure sensors as parameters to modify the input signal in the frequency domain. The outcome of this simulation reflects what a WindProbe would have measured when exposed to identical wind conditions. By comparing this simulated result with the original CTA measurement, we can characterize the impact tubing attenuation would have on real WindShaper flow measurements.

3. Probe displacement

The application requires that the hand-held probe is manually displaced by the operator to capture wind data u_{wind} in chosen spots of the test section. The probe displacement speed $v_{\text{displacement}}$ induce an equivalent wind velocity in the measured signal. Thus, it is required to subtract the probe displacement speed form the measured signal to extract the wind speed information from the measured signal.

$$u_{\text{wind}} = u_{\text{measured}} - v_{\text{displacement}}$$

This correction is easy to make because, by design this application requires that the probe's position and attitude is tracked in real-time by the motion tracking camera system. However, the applied correction isn't perfect for the following reasons:

1) The probe displacement dynamic isn't controlled. The operator is free to move the probe in his own way.
2) The noise in the probe position signal acquired by the motion tracking camera system is characterised by a standard deviation of 1×10^{-4} m. This noise was calculated from tracking data of a static object. A filter needs

Table 1 List of the different tubes tested in the present study.

Sample #	Material	inner diameter (mm)	outer diameter (mm)	length (mm)
1	PTFE	0.5	1.5	500
2	PTFE	0.7	1.2	500
3	PTFE	0.8	1.3	301
4				404
5				417
6				430
7				443
8				500
9	PTFE	0.8	1.6	400
10				450
11				500
12				600
13	PTFE	1	1.6	500
14				600
15				765
16				950
17	PTFE	1	2	500
18	Silicone	0.5	1.5	40
19				60
20				500
21	Silicone	0.8	2.4	500
22	Silicone	1	2	500
23	Silicone	1	4	500
24	Silicone	1.4	3.6	500
25	Polyurethane	1	2	500

to be applied to smooth probe displacement speed that's derived from the measured position signal.

3) This correction is applied in real-time which forces to use backward difference scheme to derive the probe displacement speed from the probe's position data. This introduces a phase-shift between the corrected signal.

The error in wind speed measurement induced by the displacement of the probe, $\epsilon_{\text{displacement}}$, can be expressed as a function of a_{probe}, the real-time acceleration of the probe, n the number of samples used in the moving average filter, and f the frequency of acquisition of the probe's position by the motion tracking camera system.

$$\epsilon_{\text{displacement}} = a_{\text{probe}} \frac{n}{2f}$$

For instance, considering a camera acquisition frequency of 120 Hz, a 3-sample window for the moving average filter, and a probe displacement following a sine wave with an amplitude of 100 mm and a frequency of 1 Hz, the maximum error calculated would be approximately 0.05 m/s. This example illustrates the maximum error is resulting from a relatively aggressive probe displacement.

Table 2 Probe measurement characteristics

Measurement characteristics	Value	Units
Max wind speed	23	m/s
Speed accuracy at 2.8 m/s	±3	%
Speed accuracy at 23 m/s	±1.6	%
Maximum flow angle	40	deg
Angle accuracy at 2.8 m/s	±0.6	deg
Angle accuracy at 23 m/s	±0.2	deg
Pressure acquisition frequency	200	Hz
Position acquisition frequency	120	Hz
Max error due to probe displacement	0.05	m/s

B. Wind profile control system

1. Measurement quality vs. scanning time

Before testing the overall efficiency of the wind profile control system, we need to quantify the minimum scanning time needed to get an accurate data capture of the velocity field across the measurement plane. For this, a reference data set was acquired during 12 min of measurements and the mean velocity in each cell of the mesh was computed. Then the same data set was gradually and randomly down sampled which virtually creates a new data set with a lower total acquisition time. The mean velocity of each cell in the down sampled data set was compared to the original one.

2. Profile generation

To test the full wind profile generator system, comprising the optically tracked probe, the Windshaper and the control software, a uniform flow profiles of 8 m/s is tested with a measurement plane parallel to the Windshaper and situated 0.1 m downstream.

To test the efficiency of that automatic system, the following procedure is applied:

1) the wind profile is setup in the graphical interface, which automatically starts the Windshaper with a "first guess" by discretizing the wind profile function in steps the size of a single fan unit and applying a linear approximation of the fan input signal (0 - 100%) vs the generated flow (0 - 16 m/s) for every fan in the Windshaper.
2) a first measurement of the test plane can be done with the probe and mean standard deviation can be plotted for this initial measurement by comparing the desired wind profile with the measured wind after the first "machine guess" across the whole test plane.
3) a scanning pass with a duration of 4 minutes per square meter of Windshaper fan area can be done. The control software will then compute a new fan control input based on this measurement to approach the desired wind profile.
4) before applying the new fan inputs, the probe is used again to measure the whole test plane, and the standard deviation from the desired wind profile can be computed once more for the whole area.
5) the last two steps can then be repeated until the overall error between the desired profile and the latest measurement decreases below a certain threshold.

After that, a graph of the standard deviation evolution vs the number of iterations can be plotted, which allows to quantify the time necessary to generate a wind profile with sufficient precision.

V. Results

A. Probe Capabilities

1. Flow angle and magnitude measurement error

The probe's characteristics are summarized in Table 2.

Preliminary results are showing a typical error on velocity magnitude from 3% at 2.8 m/s to 1.6% at 23 m/s. The

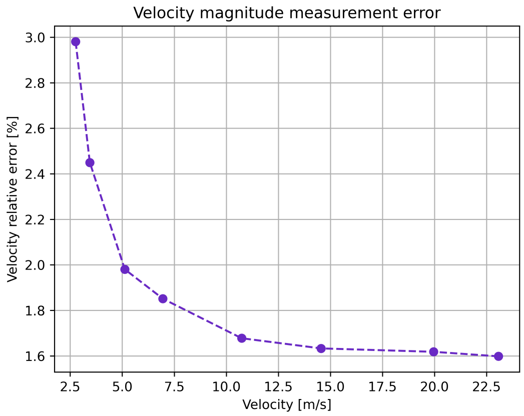

(a)

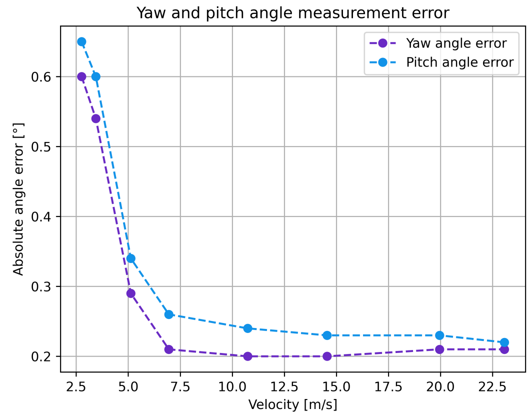

(b)

Fig. 5 (a) Relative velocity magnitude error of the velocity magnitude measured by the probe as function of the free-stream velocity magnitude. (b) Mean value of the absolute error of the angle measured by the probe as function of the free-stream velocity magnitude. The angle measurement error is averaged on the whole measurement span of ± 40° for each given velocity value.

Table 3 Comparison of the flow characteristics obtained between the CTA and the simulated WindProbe.

Flow characteristic	CTA (10 kHz)	Simulated WindProbe (200 Hz)	difference (%)
Mean velocity (m/s)	15.80	15.54	-1.7
Turbulence intensity (%)	4.93	4.58	-0.35

relative error on the velocity magnitude is visible in the figure 5a. Concerning the error in the angle measurement, a similar error in the pitch and yaw angle was observed. An absolute 0.6° error in both pitch and yaw angle is obtained at 2.8 m/s on the whole measurement span of ± 40°. The error drops to respectively 0.22° and 0.21° for the pitch and yaw angle at 23 m/s. The error trend, which is similar to the velocity magnitude's one is visible in the figure 5a. Overall the probe showed a great capability to measure the flow flied with an accuracy that should allow its data to be used by a control algorithm in order to regulated the flow field generated by a Windshaper.

2. Frequency Response

Looking at the frequency sweep results from all the 500 mm tubes tested (see Figure 6a), one can see the presence of damping in the tubes, with a complex dependence on inner and outer diameters and tube materials.

The tubes can be classified in three main groups: the first group includes tubes with significant damping (tubes 1, 7 and 2 in Figure 6a), the second group includes those with acceptable damping (tubes 3 and 4 in Figure 6a), while the third group includes tubes where amplification is observed due to wave reflections (tubes 5, 6, 8, 9, 10, 11 and 12 on Figure 6a). The tube 3 (PTFE tube with an inner diameter of 0.8 mm and an outer diameter of 1.3 mm) best met our requirements. This tube offers an absence of attenuation up 70 Hz followed by a steady decline from 70 to 200 Hz, with an attenuation of 1.3 dB at 100 Hz.

As explained in Section IV.A.2, a 150 s flow sample was acquired with a CTA probe at 1.5 m downstream of a WindShaper running at 95% PWM on all fans. After running a Fast Fourier Transform (FFT) on the initial signal, we multiplied the power at each frequency by the attenuation gain of our chosen tube, adjusting the CTA measurement according to the tube's characteristics. We then performed an inverse-FFT and downsampled the signal from 10'000 Hz to 200 Hz to obtain a simulation of what the original measurement would have looked like if taken with a WindProbe. We then compared some of the flow characteristics (mean velocity, turbulence intensity) between the original measurement and the probe's simulated measurement as well as their turbulence spectrum to assess its performance. Looking at the flow characteristics (see Table 3) one can see that the influence of the tubing on actual flow measurement is minimal.

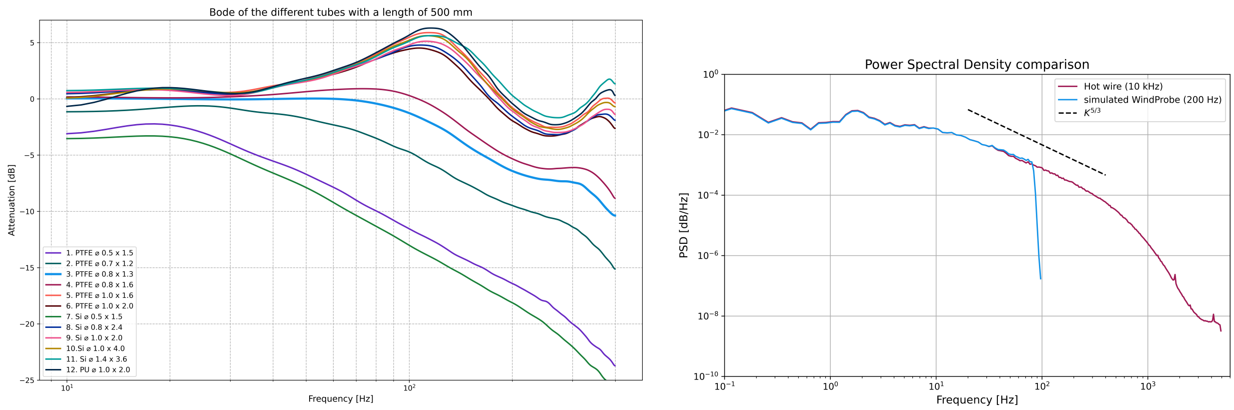

(a) **(b)**

Fig. 6 (a) Bode magnitude plot of the 500 mm long tubes tested, illustrating the frequency response of our probe. (b) Power Spectral Density (PSD) comparison of the CTA measurement (in purple) and the simulated WindProbe measurement (in blue). The two signals are very similar up to 85 Hz, showing that the probe could be capable of resolving at least part of the inertial range. Furthermore, by knowing the tubing attenuation, it is then possible to correct the signal between 50 and 200 Hz to ensure accurate results.

Furthermore, we could imagine also using the WindProbe for large-scale turbulence measurement (the probe is theoretically capable of measurements up to 1000 Hz), and apply a correction to these measurements by using the known attenuation profile of our system.

Overall, we can conclude this section by confirming that the PTFE tubes chosen to be used in the WindProbe are adequate. Their frequency response is perfectly flat up to 70 Hz and then declines steadily up to 200 Hz. The attenuation on the signal between 70 and 200 Hz is actually negligible in a real-life scenario, showing no perceptible influence on the measured flow velocity.

3. Probe displacement

Concerning the probe displacement error, it has not been assessed yet as it required a precise and controllable way to generate a set of known displacement (as it can be done with a robotic arm) in order to compare the correction velocity derived from the optically tracked position of the probe with its actual velocity. Nevertheless estimation of velocity error made in section IV.A.3 showed that we should except velocity errors lower than 0.05 m/s if the probe is moved in the flow field at a fast rate.

B. Flow control system

1. Measurement quality vs. scanning time

It was observed (see Figure 7a) that removing 80% of the data set would still allow to reconstruct the mean velocity in each cell which deviates from 1.5 % compared to the original data set. Which means that it could be possible to reach a sufficient measurements time of less than 3 minutes.

2. Profile generation

Preliminary results showed a decrease of absolute mean error from each mesh cell average velocity as new iterations of measurement and correction step were applied. The initial mean error was near 1 m/s, which after 4 correction iterations based on each 4 minutes of flow measurement, was reduce to 0.2 m/s as visible in the figure 7b. Due to restrictions on the available time, it was not possible to test different flow field nor varying flow field intensities. Still, this preliminary results showed a converging trend in the correction of the flow field generated by the Windshaper. A more in depth study of the optimal gain that could be applied to the correction algorithm could allow to reach a faster and more accurate generation of flow field profile.

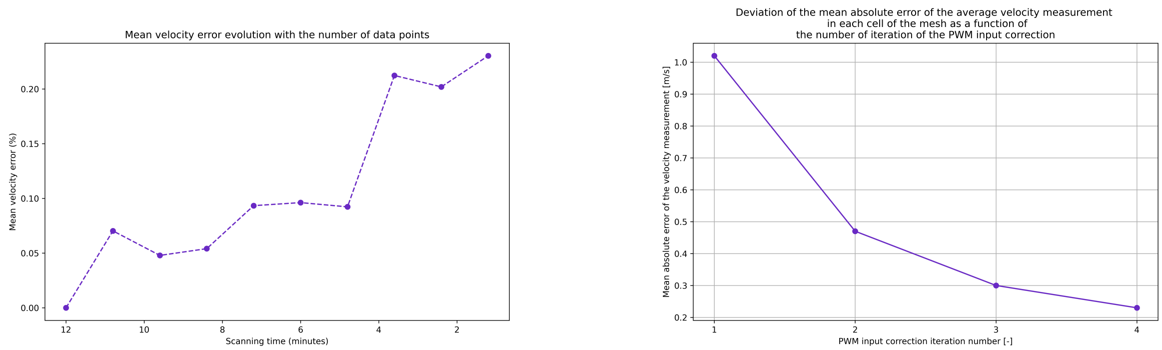

(a) **(b)**

Fig. 7 (a) Evolution of the mean measurement error across the 36 fans with scanning time. From a baseline scan of 12 minutes (52 minutes per square meter), the number of data points was reduced and the mean velocity measured across all fans was compared to the baseline measurement. The difference in percent is then plotted in absolute value. (b) Evolution of the absolute mean error on an uniform 8 m/s wind profile as function of the number of iteration done with the correction algorithm.

VI. Conclusion

The objective was to automate and simplify the flow profile control of a Windshaper fan array. First, an optically tracked 5-hole probe was designed, built and calibrated in-house. The internal design and calibration procedure were optimized to deliver accurate 3D flow velocity measurement in handheld operation at a high sampling rate. Once the probe capabilities were assessed, a control software with a GUI was developed to assist users in setting up a wind profile and seeing probe measurements displayed in real-time in a virtual duplicate of the measurement environment. This software also manages all the data from the probe and the motion tracking system, and adjusts the fan power input to reach the desired wind profile.

A first series of preliminary measurements was performed, and allowed us to assess the minimum scanning time necessary as well as the basic functioning of the correction algorithm.

In the future, the correction algorithm gain should be optimized to allow for faster and more accurate wind profile correction. Furthermore, mixing effect between flows from adjacent fans as well as boundary layer growth at the edges of the wind area at large distance downstream of the Windshaper should be evaluated to tweak the control algorithm and extend its operation limits.

In the long term, the WindProbe's data sampling rate could also be increased, allowing to use it as a turbulence measurement system. As the present study showed, by characterizing the flow measurement chain's frequency response, it would be possible to adjust the turbulence measurements to a more realistic value.

References

[1] Van der Hegge-Zijnen, B., "Improved Instrument for the Simultaneous Determination of the Static Pressure, the Magnitude and the Direction of Velocity of Fluids," *Proc. R. Acad. Sci. Amsterdam*, Vol. 32, 1929, pp. 658–663.

[2] Heckmeier, F. M., Iglesias, D., Kreft, S., Kienitz, S., and Breitsamter, C., "Development of unsteady multi-hole pressure probes based on fiber-optic pressure sensors," *Engineering Research Express*, Vol. 1, No. 2, 2019, p. 025023.

[3] Hall, B. F., and Povey, T., "The Oxford Probe: an open access five-hole probe for aerodynamic measurements," *Measurement Science and Technology*, Vol. 28, No. 3, 2017, p. 035004.

[4] Treaster, A. L., and Yocum, A. M., "The calibration and application of five-hole probes," Tech. rep., Pennsylvania State Univ University Park Applied Research Lab, 1978.

[5] Cogotti, A., "Car-wake imaging using a seven-hole probe," *SAE transactions*, 1986, pp. 1071–1095.

[6] Azartash-Namin, S. K., "Evaluation of low-cost multi-hole probes for atmospheric boundary layer investigation," Ph.D. thesis, Oklahoma State University, 2017.

[7] Mueller, A., "Real-Time 3D Flow Visualization Technique with Large Scale Capability," Ph.D. thesis, ETH Zürich, 2017.

[8] Eiffel, G., *La résistance de l'air et l'aviation - Expériences effectuées au Champ-de-Mars*, Dunod, Paris, 1910.

[9] Prandtl, L., *Gottingen wind tunnel for testing aircraft models*, NACA TN 66, Washington, 1920.

[10] Lewis, W. A., "Motor Control for Wind Tunnel Precision Speed Regulation for the Wind Tunnel Motor at California Institute of Technology," *Transactions of the American Institute of Electrical Engineers*, Vol. 49, No. 1, 1930, pp. 99–104.

[11] Espinoza, K., Valera, D. L., Torres, J. A., López, A., and Molina-Aiz, F. D., "An auto-tuning PI control system for an open-circuit low-speed wind tunnel designed for greenhouse technology," *Sensors*, Vol. 15, No. 8, 2015, pp. 19723–19749.

[12] Buggele, A. E., and Decker, A. J., "Control of wind tunnel operations using neural net interpretation of flow visualization records," *Ohio Area Net Workshop*, 1994.

[13] Dahlgren, D. M., and Chabaan, R., "Feedforward algorithm: Wind tunnel airspeed control," *2009 IEEE Vehicle Power and Propulsion Conference*, IEEE, 2009, pp. 1105–1109.

[14] Zhang, J., and Wen, L., "Wind Tunnel Wind Speed Control System Based on PLC Fuzzy Algorithm," *Journal of Physics: Conference Series*, Vol. 2037, IOP Publishing, 2021, p. 012009.

[15] Nott, C. R., Ölçmen, S. M., Lewis, D. R., and Williams, K., "Supersonic, variable-throat, blow-down wind tunnel control using genetic algorithms, neural networks, and gain scheduled PID," *Applied Intelligence*, Vol. 29, 2008, pp. 79–89.

[16] Nishi, A., and Miyagi, H., "Computer-controlled wind tunnel for wind-engineering applications," *Journal of wind engineering and industrial aerodynamics*, Vol. 54, 1995, pp. 493–504.

[17] Noca, F., Bujard, T., Visvaratnam, G., Catry, G., and Bosson, N., "Flow Profiling in a WindShaper for Testing Free-Flying Drones in Adverse Winds," *AIAA AVIATION 2021 FORUM*, 2021, p. 2577.

[18] Strom, G. H., and Halitsky, J., "Important considerations in the use of the wind tunnel for pollution studies of power plants," *Air Repair*, Vol. 4, No. 2, 1954, pp. 24–30.

[19] Noca, F., and Catry, G., "Wind generation means and wind test facility comprising the same," , Mar. 30 2017. US Patent 10,962,441.

[20] Walpen, A., Catry, G., and Noca, F., "Real-Scale Atmospheric Wind and Turbulence Replication using a Fan-Array for Environmental Testing and UAV/AAM Validation," *AIAA SCITECH 2023 Forum*, 2023, p. 0812.

[21] Govoni, T., Walpen, A., Bosson, N., Catry, G., and Noca, F., "Continuous Stochastic Data Acquisition for Improved Calibration of Multi-Hole Pressure Probes in Flow Measurements," *Bulletin of the American Physical Society*, 2023.